BIOCHEMISTRY
including biophysical chemistry & molecular biology

Article

pubs.acs.org/biochemistry

Four-State Folding of a SH3 Domain: Salt-Induced Modulation of the Stabilities of the Intermediates and Native State

Amrita Dasgupta and Jayant B. Udgaonkar*

National Centre for Biological Sciences, Tata Institute of Fundamental Research, Bangalore 560065, India

ABSTRACT: Unstable intermediates on the folding pathways of proteins can be stabilized sufficiently so that they accumulate to detectable extents by the addition of a suitable cosolute. Here, the effect of sodium sulfate (Na_2SO_4) on the folding of the SH3 domain of PI3 kinase was investigated in the presence of guanidine hydrochloride (GdnHCl) using intrinsic tyrosine fluorescence and 1-anilinonaphthalene-8-sulfonate (ANS) binding. The free energy of unfolding in water of the native state (N) increases linearly with Na_2SO_4 concentration, indicating stabilization via the Hofmeister effect. The addition of 0.5 M Na_2SO_4 causes accumulation of an early intermediate L, which manifests itself as (1) a sub-millisecond change in tyrosine and ANS fluorescence and (2) a curvature in the chevron plot. It is shown that L is a specific structural component of the initially collapsed ensemble. An intermediate, M, also accumulates in unfolding studies conducted in the presence of 0.5 M Na_2SO_4 and manifests itself by causing a curvature in the unfolding arm of the chevron. M is shown to be a wet molten globule that binds to ANS under unfolding conditions and is stabilized to the same extent as N in the presence of Na_2SO_4. A four-state U ↔ L ↔ M ↔ N scheme satisfactorily modeled the kinetic data. Thus, the folding of the PI3K SH3 domain in the presence of salt commences via the formation of a structured intermediate ensemble L, which accumulates before the rate-limiting step of folding. L subsequently proceeds to N via the late intermediate M that forms after the rate-limiting transition of folding.

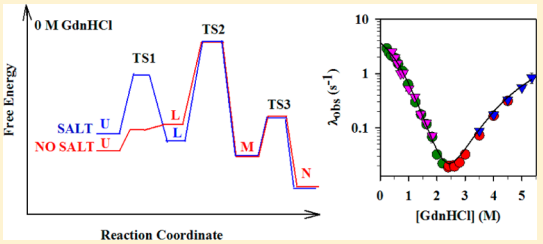

Protein folding reactions often appear to be two-state transitions between the unfolded (U) and native (N) states.[1] For such "two-state" folders, native state topology appears to be a major determinant of folding rates,[2−4] although the size of the protein[5,6] and its stability[7] also appear to be important. Mutational[8,9] and theoretical[10−12] studies suggest that transition states are predominantly native-like with few non-native interactions. This simplistic picture of protein folding is supported by and in turn reinforces simplified computer simulations of folding based on Gō models, which favor only native contacts.[13,14] The complexity of the free energy landscape available to a protein for folding[15] does, however, manifest itself in experimental studies designed to look for conformational heterogeneity,[16−20] multiple pathways,[21−25] or global downhill folding.[26−28] In contrast to barrier-limited folding where distinct structural forms are separated by substantial ($>3k_BT$) free energy barriers, global downhill folding[27,28] is a scenario in which one form changes structure gradually over many small distributed barriers.[29,30] This complexity of protein folding reactions has been captured well in recent computer simulations,[31−35] especially those based on network models.[36,37]

The hidden complexity of protein folding reactions can be revealed not only by the use of suitable experimental probes[38−41] but also by manipulation of either the folding conditions[42−44] or the protein sequence.[45,46] Such manipulation can lead to sufficient stabilization of a folding intermediate so that it is detectable.[42,47−49] Alternatively, different components of an intermediate ensemble may be stabilized under different folding conditions,[42,50] so that the ensemble-averaged structure of the intermediate will appear different under different folding conditions. Hence, the modulation of folding conditions can provide valuable insight into protein folding mechanisms. The detection and characterization of refolding and unfolding intermediates are also essential in the context of their possible role as monomeric precursors on the aggregation pathways of some proteins.[51,52]

While the role of collapsed intermediates detected before the rate-limiting step of the folding pathway is primarily to guide the unfolded state to the native protein,[53] the detection and characterization of partially unfolded forms during unfolding reactions provide insight into the chemical forces that maintain the integrity of the folded structure[54] as well as the structure of the transition state of unfolding that may or may not be similar to that of the native state.[55−57] Thus, unfolding studies of several proteins have been performed to characterize such partially unfolded forms,[20,57−59] and high-resolution probes such as hydrogen exchange[60] coupled to either NMR,[61] mass spectrometry (HX-MS),[20,58] or time-resolved (TR) multisite FRET[54] have helped in elucidating which parts of the native structure dissolve first during the unfolding process.

The PI3K SH3 domain is an 82-residue protein whose structure is composed of five β-strands and two helix-like turns (Figure 1). Earlier, SH3 domains appeared to be two-state folding proteins: kinetic intermediates could not be detected on either the folding or unfolding pathways.[1,62] Only recently have

Received: February 17, 2012
Revised: May 11, 2012
Published: May 30, 2012

   dx.doi.org/10.1021/bi300223b | *Biochemistry* 2012, 51, 4723−4734

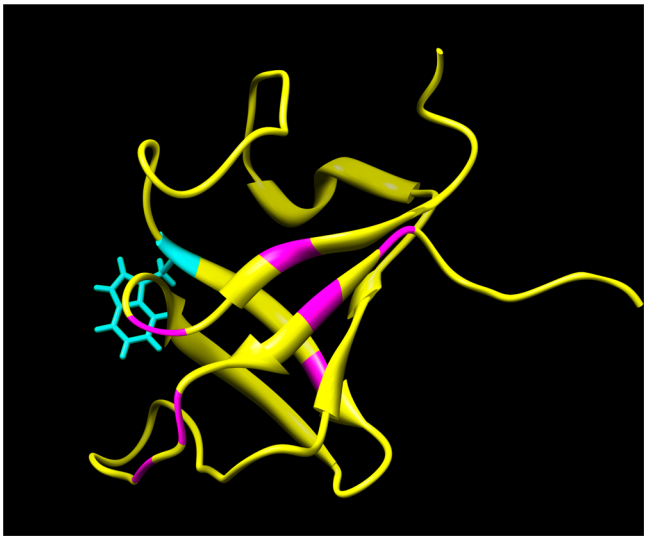

Figure 1. Structure of the PI3K SH3 domain. The positions of W53 (cyan) and the seven tyrosines (magenta) at positions 4, 6, 10, 12, 57, 71, and 74 are indicated. The ribbon diagram generated from Protein Data Bank entry 1pnj was produced using UCSF Chimera from the Resource for Biocomputing, Visualization, and Informatics at the University of California (San Francisco, CA).[102]

the folding and unfolding mechanisms of the PI3K SH3 domain been investigated in detail.[20,41,57] The refolding of the PI3K SH3 domain in the absence of added cosolutes has been shown to commence with the formation of a non-specific structure-less globule, U_C,[41] populated before the rate-limiting step of folding. Thus, this protein serves as a good model system for investigation of the interplay of collapse and structure formation in the very fast steps of protein folding and for investigation of whether the modulation of folding conditions can lead to the transformation of the collapsed product from a non-specific globule to a structured intermediate.

In this study, the effect of Na_2SO_4 on the stability of the PI3K SH3 domain and folding mechanism has been investigated. Two spectroscopic probes, intrinsic tyrosine fluorescence and ANS fluorescence, sensitive to the detection of specific intermediates, have been used to study the folding mechanism. The native state (N) is shown to become stabilized in the presence of Na_2SO_4. An intermediate (part of the collapsed ensemble) L is populated significantly in the presence of 0.5 M Na_2SO_4. When the unfolding reaction was monitored in the presence of 0.5 M Na_2SO_4, the previously identified unfolding intermediate, M,[57] was found to be stabilized to the same extent as N. Thus, in the presence of 0.5 M Na_2SO_4, the folding mechanism of the PI3K SH3 domain can be described by a linear four-state mechanism, U ↔ L ↔ M ↔ N, where L is a productive on-pathway intermediate that guides the structure-less globule U_C (the unfolded state under native-like conditions) to develop into the native state via the formation of a late folding intermediate, M.

MATERIALS AND METHODS

Protein Expression, Purification, and Labeling. The wild-type protein was purified as described previously.[41,57] Electrospray ionization mass spectrometry showed that the protein had the expected mass of 9276.2 Da.

Buffers, Reagents, and Experimental Conditions Used. All reagents and buffers, including Na_2SO_4, of the highest purity were procured from Sigma. Ultrapure grade GdnHCl and urea were obtained from USB Corp. Phosphate buffer (20 mM, pH 7.2) was included in the buffers used for all the experiments, which were all performed at 25 °C. The concentrations of the stock solutions of GdnHCl and urea were determined by refractive index measurements on an Abbe refractometer. The concentration of the wild-type protein was determined by measurement of the absorbance at 280 nm using an ε of 17900 M^{-1} cm^{-1}.[63]

For equilibrium unfolding experiments using fluorescence as the probe, the protein concentrations used were 10−15 μM. For experiments using far-UV CD at 222 nm as the probe, the concentration of the protein was 30 μM. For the kinetic refolding or unfolding experiments in the presence of 0.5 M Na_2SO_4, using tyrosine fluorescence as the probe, the concentration of the protein used was 10−20 μM. To check that transient aggregation did not occur during folding or unfolding, refolding in 0.4 M GdnHCl and unfolding in 3.5 M GdnHCl were also studied using a protein concentration of 200 μM.

Equilibrium Unfolding Experiments. Experiments at different concentrations of Na_2SO_4 were performed on a stopped-flow module (SFM-4, Biologic) in a fluorescence cuvette with a path length of 1 cm. The wavelength used for the selective excitation of the tyrosines was 268 nm, with a bandwidth of 4 nm. The fluorescence emission was measured through a 300 nm band-pass filter with a bandwidth of 10 nm (Asahi Spectra). Far-UV CD experiments were performed on a Jasco J-815 CD spectropolarimeter. A 0.2 cm path length cuvette was used for all CD experiments.

Kinetic Refolding and Unfolding Experiments. All tyrosine fluorescence and ANS fluorescence experiments were performed on the SFM-4 stopped-flow module. Typically, a dead time of 6 ms was achieved with a cuvette with a path length of 0.15 cm. For experiments using ANS, the ANS concentration was 540 μM in the refolding/unfolding buffer and the protein concentration was 45 μM.[41] The excitation wavelength was 295 nm with a bandwidth of 4 nm, and the emission wavelength was 450 nm with a bandwidth of 25 nm.

Data Analysis. *Analysis of Equilibrium and Pre-Equilibrium Unfolding Data.* The equilibrium data for the unfolding of N to U (the N ↔ U transition), the t = 0 points of the kinetic traces of refolding (the U ↔ L transition) and unfolding (the N ↔ M transition) as a function of the concentration of GdnHCl, [D], at a fixed concentration of Na_2SO_4, [S], were fit to a two-state i ↔ j model given by the following equation:

$$Y_0 = \left[Y_i + m_i^S[D] + (Y_j + m_j^S[D])e^{-(\Delta G_{ij}^{o,S} + m_{ij}^S[D])/RT}\right] \Big/ \left[1 + e^{-(\Delta G_{ij}^{o,S} + m_{ij}^S[D])/RT}\right] \quad (1)$$

where Y_0 is the value of the spectroscopic property being measured as a function of [D], Y_i and Y_j represent the intercepts, m_i^S and m_j^S represent the slopes of the pre- and post-transition baselines for the i ↔ j transition, respectively, $\Delta G_{ij}^{o,S}$ is the free energy of unfolding of state i in water at a fixed concentration of Na_2SO_4, and m_{ij}^S is the change in the free energy associated with the preferential interaction of D with state j, relative to state i.

The raw data for the equilibrium unfolding of N to U at different concentrations of S were also converted to plots of f_U versus [D] using eq 2 and then fit to eq 3:

$$f_U = \frac{Y_0 - (Y_N + m_N^S[D])}{Y_U + m_U^S[D] - (Y_N + m_N^S[D])} \quad (2)$$

$$f_U = \frac{e^{-(\Delta G_{NU}^{o,S} + m_{NU}^S[D])/RT}}{1 + e^{-(\Delta G_{NU}^{o,S} + m_{NU}^S[D])/RT}} \quad (3)$$

The data in Figure 3A were fit to the expression given below

$$\Delta G_{NU}^{o,S} = \Delta G_{NU}^{o} + m_S[S] \quad (4)$$

where ΔG_{NU}^{o} is the free energy of unfolding of N in the absence of any salt and m_S is the change in free energy associated with the preferential interaction of Na_2SO_4 with U, relative to N in the absence of any denaturant.[42]

Analysis of the Refolding and Unfolding Kinetics in the Presence of 0.5 M Na_2SO_4. The refolding and unfolding kinetics in Figure 5 were analyzed according to Scheme 1.

Scheme 1

$$U \underset{k_{LU}^S}{\overset{k_{UL}^S}{\rightleftharpoons}} L \underset{k_{ML}^S}{\overset{k_{LM}^S}{\rightleftharpoons}} M \underset{k_{NM}^S}{\overset{k_{MN}^S}{\rightleftharpoons}} N$$

The free energies for unfolding when [S] = 0.5 M Na_2SO_4, ΔG_{LU}^S, ΔG_{ML}^S, and ΔG_{NM}^S, were assumed to be linearly dependent on [D], given by the slopes m_{LU}^S, m_{ML}^S, and m_{NM}^S, respectively.

$$\Delta G_{LU}^S = \Delta G_{LU}^{o,S} + m_{LU}^S[D] \quad (5)$$

$$\Delta G_{ML}^S = \Delta G_{ML}^{o,S} + m_{ML}^S[D] \quad (6)$$

$$\Delta G_{NM}^S = \Delta G_{NM}^{o,S} + m_{NM}^S[D] \quad (7)$$

where $\Delta G_{LU}^{o,S}$, $\Delta G_{ML}^{o,S}$, and $\Delta G_{NM}^{o,S}$ are the free energies of unfolding in 0.5 M Na_2SO_4 in the absence of a denaturant.

Two-state analyses (see above) were performed to obtain the values of $\Delta G_{LU}^{o,S}$ and m_{LU}^S, and $\Delta G_{NM}^{o,S}$ and m_{NM}^S, from the dependencies on [D] of the t = 0 points of the kinetic traces of refolding and unfolding in Figure 4, respectively. Then, the values of $\Delta G_{ML}^{o,S}$ and m_{ML}^S were obtained from eqs 8 and 9:[64,65]

$$\Delta G_{NU}^{o,S} = \Delta G_{NM}^{o,S} + \Delta G_{ML}^{o,S} + \Delta G_{LU}^{o,S} \quad (8)$$

$$-m_{NU}^S = -m_{NM}^S - m_{ML}^S - m_{LU}^S \quad (9)$$

The microscopic rate constants, k_{LM}^S and k_{ML}^S (in Scheme 1), are defined as

$$\ln k_{ML}^S = \ln k_{ML}^{o,S} + m_{ML}^{k,S}[D]/RT \quad (10)$$

$$\ln k_{LM}^S = \ln k_{LM}^{o,S} + m_{LM}^{k,S}[D]/RT \quad (11)$$

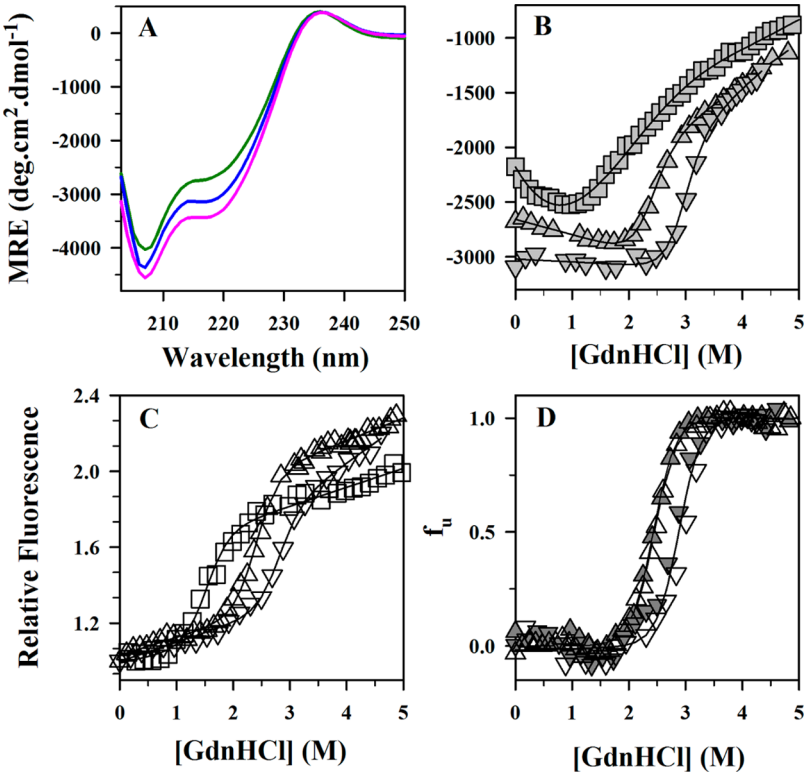

Figure 2. Dependence of the structure and stability of the PI3K SH3 domain on Na_2SO_4 concentration at pH 7.2 and 25 °C monitored by intrinsic tyrosine fluorescence and far-UV CD. (A) Far-UV CD spectra in 0 M (green), 0.5 M (blue), and 1.0 M Na_2SO_4 (pink). (B and C) Equilibrium GdnHCl-induced unfolding transitions monitored using far-UV CD at 222 nm (B) (filled symbols) and intrinsic tyrosine fluorescence at 300 nm (C) (empty symbols) in the presence of 0 M (squares), 0.5 M (triangles), and 1.0 M Na_2SO_4 (inverted triangles). The solid lines in panels B and C represent fits to a two-state N ↔ U model for unfolding using eq 1. The fit yields values for the midpoint of the transition, C_m^S, and for the free energy of unfolding, $\Delta G_{NU}^{o,S}$, of 1.4 M and 4.2 kcal mol^{-1} at [S] = 0; 2.3 M and 7.1 kcal mol^{-1} at [S] = 0.5 M Na_2SO_4; and 3 M and 9.3 kcal mol^{-1} at [S] = 1.0 M Na_2SO_4, respectively. The raw data in panels B and C were transformed into plots of f_u vs [GdnHCl] using eq 2, which are shown in panel D. Data obtained using intrinsic tyrosine fluorescence (empty symbols) and MRE at 222 nm (filled symbols) as the probes for unfolding in 0.5 M (triangles) and 1 M Na_2SO_4 (inverted triangles) are shown. The solid lines through the data in panel D represent fits to eq 3.

dx.doi.org/10.1021/bi300223b | *Biochemistry* 2012, 51, 4723−4734

where $k^{o,S}_{ML}$ and $k^{o,S}_{LM}$ are the values in 0.5 M Na_2SO_4 and $m^{k,S}_{ML}$ and $m^{k,S}_{LM}$ represent the preferential free energies of interaction with denaturant, of TS2 (the transition state preceding M during folding) in comparison to that of M, and that of L, respectively.

The sequential four-state model (Scheme 1) was used to analyze the observed refolding and unfolding kinetics in Figure 5. The analytical solution to Scheme 1 is complex. To make the analyses simple, we assumed that k^S_{UL} and k^S_{LU} are greater than k^S_{LM} and that k^S_{MN} and k^S_{NM} are greater than k^S_{ML} for all concentrations of denaturant. Thus, during refolding, U rapidly transforms to L and a fast pre-equilibrium can be assumed for the U ↔ L transition.[53] Similarly, during unfolding, N rapidly transforms to M and a fast pre-equilibrium can be assumed for the N ↔ M transition.[57] The equilibrium constants defining the pre-equilibrium for the refolding and unfolding reactions are defined by $K^S_{UL} = k^S_{UL}/k^S_{LU}$ and $K^S_{NM} = k^S_{NM}/k^S_{MN}$, respectively, where $\Delta G^S_{UL} = -RT \ln(K^S_{UL})$ and $\Delta G^S_{NM} = -RT \ln(K^S_{NM})$. For the refolding reaction, the major observable phase is the transition from L to N via M. Thus, the observed rate constant for refolding, λ_f, can be approximated by the equation

$$\lambda_f = \frac{K^S_{UL}}{K^S_{UL} + 1} k^S_{LM} \tag{12a}$$

Under refolding conditions, M is very rapidly transformed to N, and the transition from U to N via L can therefore be approximated as a three-state reaction.[47,64] At high GdnHCl concentrations, $K^S_{UL} \ll 1$ and

$$\lambda_f = K^S_{UL} k^S_{LM} \tag{12b}$$

Using a similar analysis for the unfolding reaction, where the single phase observed during unfolding is the transition from M to U via L, the observed rate constant for unfolding, λ_u, is approximated by the equation

$$\lambda_u = \frac{K^S_{NM}}{K^S_{NM} + 1} k^S_{ML} \tag{13a}$$

Under unfolding conditions, L is rapidly transformed to U, and therefore, the transition from N to U via M can be considered to approximate a three-state transition.[57] At low GdnHCl concentrations, $K^S_{NM} \ll 1$ and

$$\lambda_u = K^S_{NM} k^S_{ML} \tag{13b}$$

From eqs 12b and 13b, $K^S_{NU} = \lambda_u/\lambda_f$ or $K^S_{NU} = (K^S_{NM}K^S_{ML})/K^S_{UL}$.

Because curvatures were observed in the refolding and unfolding chevrons, the dependence of λ_{obs} on GdnHCl concentration was fit to the equation $\lambda_{obs} = \lambda_f + \lambda_u$. Hence

$$\lambda_{obs} = \frac{K^S_{UL}}{K^S_{UL} + 1} k^S_{LM} + \frac{K^S_{NM}}{K^S_{NM} + 1} k^S_{ML} \tag{14}$$

or

$$\lambda_{obs} = \frac{K^{o,S}_{UL} e^{-m^S_{UL}[D]/RT}}{K^{o,S}_{UL} e^{-m^S_{UL}[D]/RT} + 1} \times k^{o,S}_{LM} \times e^{m^{k,S}_{LM}[D]/RT} + \frac{K^{o,S}_{NM} e^{-m^S_{NM}[D]/RT}}{K^{o,S}_{NM} e^{-m^S_{NM}[D]/RT} + 1} \times k^{o,S}_{ML} \times e^{m^{k,S}_{ML}[D]/RT} \tag{15}$$

where $K^{o,S}_{UL}$ and $K^{o,S}_{NM}$ are equilibrium constants defining the pre-equilibrium for the refolding and unfolding reactions, respectively, in the presence of 0.5 M Na_2SO_4 and in the absence of any denaturant.

RESULTS

Spectroscopic Characterization of the PI3K SH3 Domain in the Presence of Na_2SO_4. Upon addition of Na_2SO_4, the fluorescence emission spectrum of the native protein shows no change in its λ_{max} or intensity (data not shown). However, the far-UV CD spectrum (Figure 2A) of the native protein shows an increase in the MRE at 222 nm with an increase in the concentration of Na_2SO_4. It is important to note that the protein remains monomeric at high concentrations of Na_2SO_4. Dynamic light scattering (DLS) experiments as well as multiple-angle light scattering (MALS) experiments conducted at a 10-fold higher protein concentration (150 μM) show that the native protein has the same hydrodynamic radius and molar mass in 0.5 M Na_2SO_4 that it does in the absence of added salt (data not shown).

Panels B and C of Figure 2 show the GdnHCl-induced equilibrium transitions at varying concentrations of Na_2SO_4 using far-UV CD at 222 nm and intrinsic tyrosine fluorescence at 300 nm, respectively, as the probes. The results obtained in the absence of Na_2SO_4 are the same as those reported previously.[41,57,62] The far-UV CD-monitored GdnHCl-induced unfolding transitions of the protein in 0.5 and 1.0 M Na_2SO_4 are distinctly sigmoidal compared to the transition in the absence of Na_2SO_4. The sigmoidal GdnHCl-induced equilibrium unfolding transitions obtained in the presence of Na_2SO_4 using the two probes were found to be completely coincident (Figure 2D). Hence, a concomitant loss of secondary and tertiary structure occurs in the presence of salt, validating the assumption made in the analysis using eq 1, that the N ↔ U transition is essentially two-state with no intermediate detectable at equilibrium.

Fluorescence emission-monitored GdnHCl-induced and far-UV CD-monitored GdnHCl-induced equilibrium unfolding experiments were performed at different concentrations of Na_2SO_4 (Figure 3A,B). Fluorescence-monitored urea-induced equilibrium unfolding transitions at varying concentrations of Na_2SO_4 were also examined (Figure 3A). Identical values are obtained for $\Delta G^{o,S}_{NU}$ from the urea-induced and GdnHCl-induced equilibrium unfolding experiments at different Na_2SO_4 concentrations (Figure 3A), indicating that the ionic strength of GdnHCl does not contribute to the enhanced stability of the protein in the presence of Na_2SO_4. The value of the free energy for unfolding, $\Delta G^{o,S}_{NU}$ (see Data Analysis), and the midpoint of the transition (C_m) are seen to increase linearly with an increase in [S]. The value of m^S_{NU} (a measure of the change in accessible solvent surface area) did not change significantly with the addition of Na_2SO_4; thus, average values of −3.0 ± 0.3 kcal mol^{-1} M^{-1} in GdnHCl and −1.1 ± 0.05 kcal mol^{-1} M^{-1} in urea were used for all the analyses.

Intrinsic Tyrosine Fluorescence-Monitored Refolding and Unfolding Kinetics. Panels A and B of Figure 4 show representative kinetic traces of refolding and unfolding, respectively, in the presence of 0.5 M Na_2SO_4. In both the refolding and unfolding kinetics, a burst phase (within 6 ms of mixing) is observed (Figure 4C); the $t = 0$ points of the kinetic traces of refolding and unfolding do not fall on the extrapolated unfolded and native baselines, respectively. Refolding subsequent to the burst phase occurs in two exponential phases at <2

dx.doi.org/10.1021/bi300223b | Biochemistry 2012, 51, 4723−4734

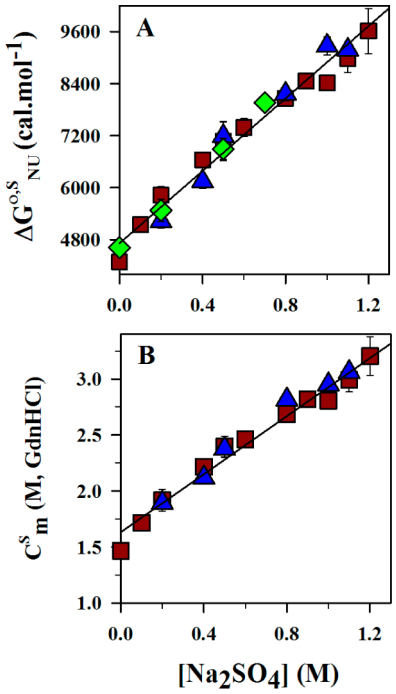

Figure 3. Effect of Na_2SO_4 on the free energy of unfolding of the PI3K SH3 domain. $\Delta G^{o,S}_{NU}$ (A) and C^S_m (B) were determined for the GdnHCl-induced unfolding transitions using intrinsic tyrosine fluorescence at 300 nm (brown squares) and MRE at 222 nm (blue triangles) as the probes at different concentrations of Na_2SO_4. Panel A also shows the effect of Na_2SO_4 on $\Delta G^{o,S}_{NU}$ (green diamonds) determined for urea-induced unfolding transitions using tyrosine fluorescence at 300 nm. Mean values for m^S_{NU} of −3.0 kcal mol^{-1} M^{-1} in GdnHCl and −1.1 kcal mol^{-1} M^{-1} in urea were used in the two-state fitting analysis. The solid line in panel A represents a fit to eq 4 and that in panel B to the equation $C^S_m = C_m + 1.3[S]$. The error bars represent the standard deviations obtained from two or more independent experiments.

M GdnHCl and in a single-exponential phase at >2 M GdnHCl. The observable phase for unfolding below 4 M GdnHCl fits to a single-exponential equation. The $t = \infty$ points of the kinetic traces of refolding or unfolding lie on the equilibrium unfolding transition in Figure 4C, indicating that both reactions were monitored to completion. To rule out the possibility that transient aggregation occurs during folding or unfolding, it was important to show that the observed folding and unfolding rates were independent of protein concentration. When folding in 0.4 M GdnHCl or unfolding in 3.5 M GdnHCl was conducted at 10-fold higher protein concentrations (see Materials and Methods), it was found that the observed folding and unfolding rates were indeed not altered (data not shown).

The $t = 0$ points of the kinetic traces of refolding and unfolding in Figure 4C show sigmoidal dependencies on the GdnHCl concentration. Thus, the burst phase change during refolding suggests that a rapid pre-equilibrium is established initially between U and a refolding intermediate, L, during refolding. Similarly, the unfolding kinetics suggests that a rapid pre-equilibrium is established between N and an unfolding intermediate, M, during unfolding (see Data Analysis).

ANS Fluorescence-Monitored Refolding and Unfolding Kinetics. ANS is a hydrophobic dye that binds to solvent-exposed hydrophobic clusters in folding and unfolding intermediates.[21,41,66−68] Such binding leads to an enhancement of the fluorescence signal of the bound ANS. Figure 4D shows representative kinetic traces of refolding monitored using ANS fluorescence, in the presence of 0.5 M Na_2SO_4. It is seen that the change in ANS fluorescence for the refolding reaction at the lowest concentration of GdnHCl is large and has increased substantially versus that seen for folding in the absence of salt.[41] The inset of Figure 4D shows that the amplitude of the initial increase in ANS fluorescence decreases exponentially with an increase in the concentration of GdnHCl at which folding is conducted.

When ANS fluorescence was used to monitor the unfolding of the PI3K SH3 domain in the presence of 0.5 M Na_2SO_4, an increase in fluorescence was observed (Figure 4E), which is significantly smaller than the amplitude observed during refolding. Such an increase in ANS fluorescence, with a similar amplitude, was also observed when the unfolding was conducted in the absence of added salt (data not shown). The rates of unfolding (Figure 5) at high concentrations of GdnHCl (>4 M) could be measured only using ANS fluorescence, because the entire change measured by intrinsic tyrosine fluorescence occurred in the burst phase of unfolding. The curvature in the unfolding arm of the chevron becomes clear when it is constructed with both the intrinsic tyrosine fluorescence and ANS fluorescence-monitored rate constants.

The Refolding and Unfolding Kinetics of the PI3K SH3 Domain Can Be Described Using a Minimal Four-State Scheme. Figure 4 shows that a refolding (L) and unfolding (M) intermediate can be detected in kinetic studies monitoring intrinsic tyrosine fluorescence and ANS fluorescence in the presence of 0.5 M Na_2SO_4. M represents a late intermediate ensemble that is populated in the absence[57] and presence of 0.5 M Na_2SO_4. L is detected only in the presence of 0.5 M Na_2SO_4. In Figure 5, it is shown that the ANS fluorescence-monitored rates of refolding and unfolding coincide with the rates observed using tyrosine fluorescence, indicating that both probes monitor the same kinetic process. It is seen that at low (<1 M) and high concentrations (>4 M) of GdnHCl, λ_{obs} begins to level off. Thus, the dependencies of the observed rates of the fast phase of refolding and unfolding on the GdnHCl concentration in Figure 5 were analyzed on the basis of a four-state mechanism represented by Scheme 1 (see Data Analysis). The dependence on the GdnHCl concentration of the observed folding and unfolding rate constants was fit to eq 15. The values of various parameters used in the four-state model fitting analysis are listed in Table 1.

In the analysis according to the four-state model shown in Scheme 1, the values of $\Delta G^{o,S}_{LU}$ and m^S_{LU}, as well as $\Delta G^{o,S}_{NM}$ and m^S_{NM}, were obtained by fitting the dependencies on [D] of the $t = 0$ points of the kinetic traces of refolding and unfolding in Figure 4, respectively, to eq 1. Equivalent fits were obtained when these $\Delta G^{o,S}$ and m^S values were within ±10% of the best-fit values listed in Table 1. When the $\Delta G^{o,S}$ and m^S values were varied outside this range, the fits were not satisfactory. It should be noted that the $\Delta G^{o,S}$ and m^S values we obtain for the U ↔ L and N ↔ M transitions are robust because they have been obtained from analyses of the amplitudes of the burst phase changes accompanying these transitions. The values of the various parameters listed in Table 1 could satisfactorily simulate the experimentally observed kinetic traces of refolding in 0.4 M GdnHCl as well as of unfolding in 4 M GdnHCl (simulations not shown).

dx.doi.org/10.1021/bi300223b | *Biochemistry* 2012, 51, 4723−4734

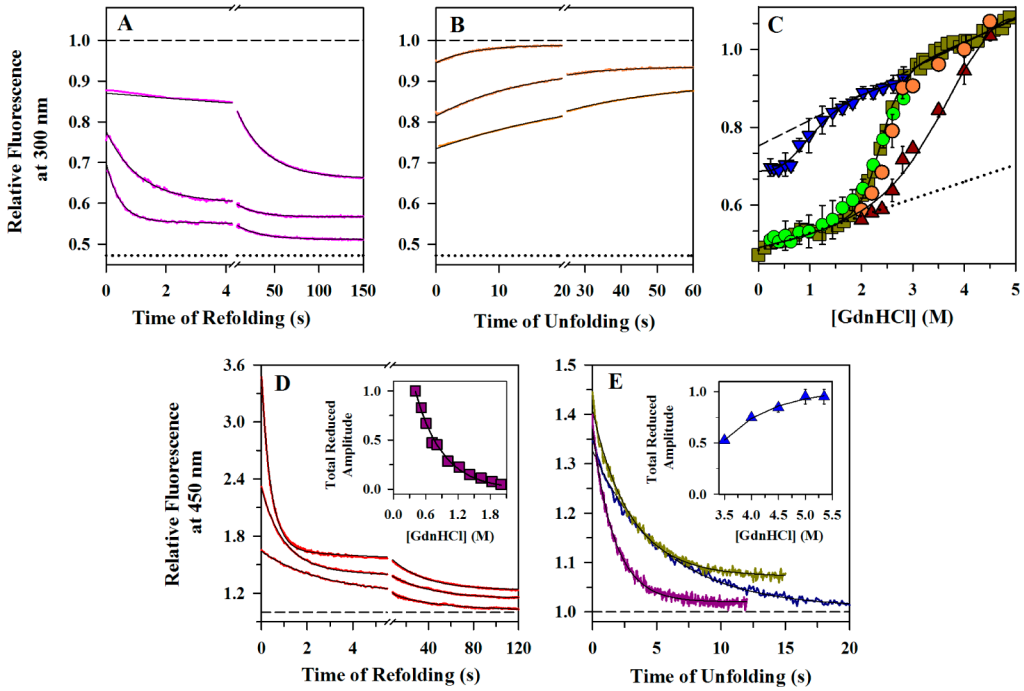

Figure 4. Refolding and unfolding kinetics of the PI3K SH3 domain in 0.5 M Na_2SO_4. Panel A shows representative kinetic traces of refolding monitored using intrinsic tyrosine fluorescence at 300 nm. Protein in 4 M GdnHCl was refolded by diluting the GdnHCl concentration to 2.0, 0.8, and 0.4 M (top to bottom, respectively). The solid lines represent double-exponential fits to the kinetic traces for refolding in 0.4 and 0.8 M GdnHCl and a single-exponential fit to the kinetic trace for refolding in 2.0 M GdnHCl. Panel B shows representative kinetic traces of unfolding monitored using intrinsic tyrosine fluorescence at 300 nm. Native protein in 0 M GdnHCl was unfolded to 4, 3.5, and 3 M GdnHCl (top to bottom, respectively). Each trace in panels A and B was normalized to a value of 1 for the fluorescence of the unfolded protein in 4 M GdnHCl, indicated by the dashed line. The solid lines in panel B represent fits to a single-exponential equation. The signal of the native protein normalized to the fluorescence of the unfolded protein in 4 M GdnHCl is indicated by the dotted lines in panels A and B. Panel C shows a comparison of the kinetic and equilibrium amplitudes for the refolding and unfolding in 0.5 M Na_2SO_4: (gray squares) equilibrium unfolding transition, (blue triangles) $t = 0$ points and (green circles) $t = \infty$ points of kinetic traces of refolding, and (brown triangles) $t = 0$ points and (orange circles) $t = \infty$ points of kinetic traces of unfolding. The solid line through the equilibrium unfolding data in panel C represents a fit to eq 1. The solid line through the $t = 0$ (blue triangles) points from the kinetic traces of refolding represents a fit to a two-state U ↔ L transition using eq 1, and the solid line through the $t = 0$ points (brown triangles) from the kinetic unfolding traces represents a fit to the two-state N ↔ M transition using eq 1. The dotted and dashed lines in panel C represent the linearly extrapolated native and unfolded baselines, respectively. Panel D shows the ANS fluorescence-monitored refolding kinetics in the presence of 0.5 M Na_2SO_4. The data show representative kinetic traces of refolding in 0.4, 0.8, and 1.2 M GdnHCl (top to bottom, respectively) in the presence of ANS starting from the unfolded protein in 4 M GdnHCl. The solid black lines through the data show fits to a single-exponential equation for the kinetic trace obtained in 1.2 M GdnHCl and to a double-exponential equation for the traces obtained in 0.4 and 0.8 M GdnHCl. The dashed line represents the ANS fluorescence of unfolded protein in 4 M GdnHCl. The inset shows the dependence of the total ANS fluorescence amplitude (maroon squares) on the concentration of GdnHCl present during refolding. The amplitudes are normalized to a value of 1 for the amplitude of the ANS fluorescence change observed for the refolding in 0.4 M GdnHCl. The solid line through the data is drawn by visual inspection only. Panel E shows the ANS fluorescence-monitored unfolding kinetics in the presence of 0.5 M Na_2SO_4. Native protein in 0 M GdnHCl was unfolded to 4 (dark blue), 4.5 (dark green), and 5 M GdnHCl (dark pink). Each trace in panel E was normalized to a value of 1 for the fluorescence of the native protein in 0 M GdnHCl, indicated by the dashed line. The solid lines in panel E represent fits to a single-exponential equation. The error bars represent the standard deviations obtained from two or more independent experiments.

DISCUSSION

Mechanism of Na_2SO_4-Induced Stabilization of the Native PI3K SH3 Domain. The structural integrity of the native state of a protein is maintained by different stabilizing interactions. These interactions are strongly influenced by a change in the external environment of the protein.[69−71] Salts are known to stabilize native states and compact intermediate states via one of the three mechanisms: ion binding, Debye screening, and the Hofmeister effect.[42,70,72,73] Hofmeister salts such as sulfates enhance protein stability by the preferential exclusion of the largely hydrated sulfate anion from the surface of the protein, resulting in an increase in the hydrophobic forces within the protein.[42,72,74]

Certain key observations support the Hofmeister effect being the major effect enhancing the stability of the native state of the PI3K SH3 domain in the presence of Na_2SO_4. (1) The linear dependence of the free energy of unfolding ($\Delta G^{o,S}_{NU}$) on Na_2SO_4 concentration supports the weak interaction model used to explain the Hofmeister effect.[42,72,74,75] The weak interaction model describes the interaction of the Hofmeister salt with the protein; the salt serves as a chemical perturbant that increases the chemical potential of the protein.[42] (2) When $\Delta G^{o,S}_{NU}$ was plotted against the logarithm of the salt concentration, curvature at high salt concentrations was observed (data not shown), contrary to the linear dependence expected for a purely cation binding effect.[76] (3) A plot of $\Delta G^{o,S}_{NU}$ versus the square root of the ionic strength is not linear (data not shown), clearly indicating that the mechanism of salt-induced stabilization in the case of the native state of the PI3K SH3 domain is not Debye screening, as has been reported in the case of the Fyn SH3 domain.[77]

dx.doi.org/10.1021/bi300223b | *Biochemistry* 2012, 51, 4723−4734

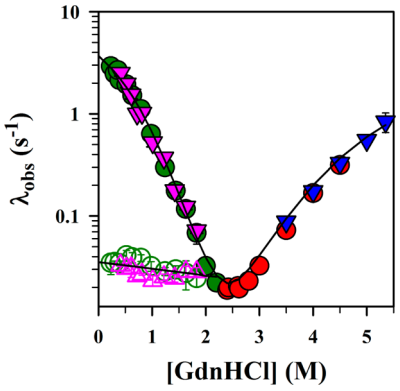

Figure 5. Dependence of the observed rate constants of the fast phase of refolding (solid green circles and solid magenta triangles), the slow phase of refolding (empty green circles and empty magenta triangles), and the fast phase of unfolding (solid red circles and solid blue triangles) using intrinsic tyrosine fluorescence at 300 nm (circles) and ANS fluorescence (triangles) as the probes. The solid line through the fast phase of refolding and unfolding is a fit to eq 15. The values of the parameters used and obtained are listed in Table 1. The solid line through the slow phase of the refolding constant data is a least-squares fit to the equation $\log \lambda^s = \log \lambda^s_{water} + m^s_f[\text{GdnHCl}]$, and a λ^s_{water} of 0.03 s^{-1} and an m^s_f of −0.01 M^{-1} were obtained. The error bars in the data points represent the standard deviations obtained from two or more independent experiments.

Stabilization of the Native State Induces Cooperativity in the Equilibrium Unfolding of the PI3K SH3 Domain. The GdnHCl-induced equilibrium unfolding of the PI3K SH3 domain monitored using far-UV CD at 222 nm shows an anomalous shape,[41,57] suggestive of a noncooperative transition from N to U. In fact, both theoretical studies[15] and studies using computer simulations[78,79] have predicted that natural proteins can fold exhibiting marginal cooperativity.

In a theoretical study, it was seen that a greater number of nonlocal contacts in the native fold gave rise to a more cooperative unfolding transition.[80] It was suggested that when the native state is stabilized predominantly by local contacts, the free energy barrier between the native and denatured states may disappear (causing a loss of cooperativity) because of the population of partially folded forms that are energetically similar to the native state (leading to a broader native basin). Such conformations that are neither U nor N may be involved in the local ordering of certain residues.[81] Deviations from a cooperative transition due to the presence of such partially folded conformations were also tested and reported in studies using a lattice model for the side chains.[79] If the native state is stabilized significantly compared to the other partially folded conformations (via a decrease in temperature or addition of a cosolute), the transition is expected to become more cooperative.[80] Nevertheless, contrary to this expectation, the small protein BBL, which has been shown to be a downhill folder,[26] shows a decrease in the cooperativity of the unfolding transition upon addition of stabilizing cosolutes.[82]

In the equilibrium unfolding of the PI3K SH3 domain, Na_2SO_4 increases the cooperativity of the transition, possibly by enhancing hydrophobic interactions within the protein that leads to the native state being energetically more stable and thus distinct from other partially folded conformations. A similar observation was reported in a study characterizing an intermediate on the folding pathway of apomyoglobin.[83]

Table 1. Parameters Describing the Folding and Unfolding of the PI3K SH3 Domain in the Presence of 0.5 M Na_2SO_4

	equilibrium	kinetics
$\Delta G^{o,S}_{NU}$ (kcal mol^{-1})	7.1 ± 0.4	7.3
m^S_{NU} (kcal mol^{-1} M^{-1})	−3.0 ± 0.3	−3.1
$\Delta G^{o,S}_{LU}$ (kcal mol^{-1})[a]		1.1
m^S_{LU} (kcal mol^{-1} M^{-1})[a]		−1.55
$K^{o,S}_{LU}$		0.16
$\Delta G^{o,S}_{NM}$ (kcal mol^{-1})[a]		3.8
m^S_{NM} (kcal mol^{-1} M^{-1})[a]		−0.9
$K^{o,S}_{NM}$		0.0016
$\Delta G^{o,S}_{ML}$ (kcal mol^{-1})[b]		2.4
m^S_{ML} (kcal mol^{-1} M^{-1})[b]		−0.7
$K^{o,S}_{ML}$		0.016
$k^{o,S}_{LM}$ (s^{-1})[c]		4.3
$k^{o,S}_{ML}$ (s^{-1})[d]		0.07
$m^{k,S}_{LM}$ (kcal mol^{-1} M^{-1})[c]		−0.43
$m^{k,S}_{ML}$ (kcal mol^{-1} M^{-1})[c]		0.28
$\alpha_L = -m^S_{LU}/-m^S_{NU}$	0.5	
$\alpha_M = -m^S_{ML} - m^S_{LU}/-m^S_{NU}$	0.7	

[a]The values for these parameters were determined from the two-state analysis of the $t = 0$ points of the kinetic refolding and unfolding traces (Figure 4C). [b]These parameters were determined from eqs 8 and 9 (see Data Analysis). [c]The values of these parameters were obtained from the fit to the dependence of λ_{obs} on the concentration of GdnHCl (Figure 5) using the four-state model in Scheme 1 (described in Data Analysis). [d]The value for $k^{o,S}_{ML}$ was fixed to obtain the best fit and to fulfill the criterion that $K^{o,S}_{ML} = 0.016$. α_L and α_M are measures of the position of L and M along the reaction coordinate relative to the position of N.[57,64]

The Folding Mechanism of the PI3K SH3 Domain Can Be Described Using a Linear Four-State Scheme. In the presence of 0.5 M Na_2SO_4, the folding mechanism of the PI3K SH3 domain appears to be described well by a minimal four-state mechanism (Scheme 1). The following observations warrant the use of the four-state scheme. (1) Burst phase changes in intrinsic tyrosine fluorescence are observed when this probe is used as the probe for both the refolding and unfolding reactions (Figure 4A–C). (2) An increase in ANS fluorescence is observed for both refolding (Figure 4D) and unfolding reactions (Figure 4E). (3) Curvatures (rollovers) are observed in the refolding and unfolding arms of the chevron plot (Figure 5).

Figure 6 shows that, when Scheme 1 is used to fit the observed rates of folding (see approximations used in Data Analysis), the rate-limiting step is the transition from L to M. Under refolding conditions in the presence of 0.5 M Na_2SO_4, the late intermediate, M, is not populated because it is less stable than N (as seen in Figure 6) and its conversion to N is much faster than its formation. On the other hand, under unfolding conditions, L remains undetected. Thus, under refolding or unfolding conditions, the folding mechanism of the PI3K SH3 domain can be approximated as a three-state model via the formation of L and M (see Data Analysis). Moreover, the rates of refolding at low concentrations of GdnHCl are enhanced in the presence of salt. This is most likely due to an increase in the stability of the native state or the early intermediate, L,[42,50] which had not been previously detected for folding in the absence of added salt.[41]

Refolding Mechanism of the PI3K SH3 Domain in the Presence of Salt. The addition of 0.5 M Na_2SO_4 to the refolding reaction gives rise to a sub-millisecond burst phase

dx.doi.org/10.1021/bi300223b | Biochemistry 2012, 51, 4723–4734

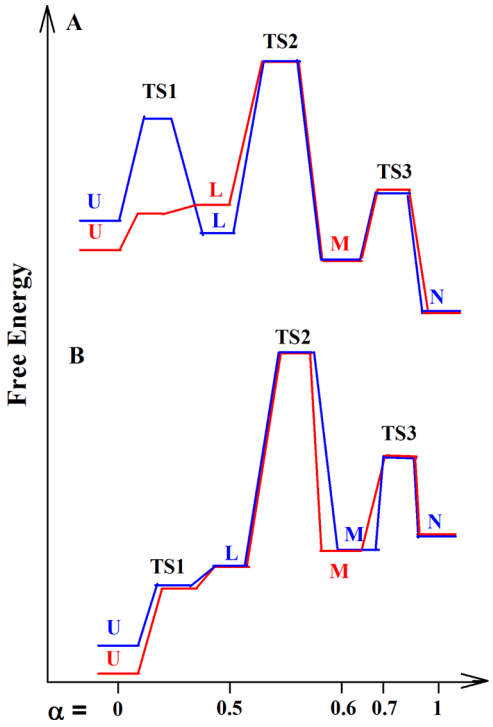

Figure 6. Free energy diagrams estimated on the basis of the thermodynamic and kinetic parameters listed in Table 1 obtained from the four-state modeling of the chevron plot. The reaction coordinate for unfolding, α_i, is a measure of the position of U, L, and M along the reaction coordinate relative to that of N. α_L and α_M are defined in Table 1, and their values are relative to an α_U of 0 and an α_N of 1. The red profiles are for folding and unfolding in the absence of salt, and the blue profiles are for folding and unfolding in the presence of 0.5 M Na_2SO_4. Panel A shows the free energy profile in 0 M GdnHCl, and panel B shows the free energy profile in 5 M GdnHCl. The free energy diagrams indicate the stabilization of L during refolding in the presence of 0.5 M Na_2SO_4.

and a rollover in the refolding limb of the chevron plot (Figure 5) that are not observed for folding in the absence of salt.[41] This observation indicates that within the mixing dead time of the refolding reaction, a rapid pre-equilibrium is established between U and an early intermediate, L. The dependence of the burst phase amplitude observed using intrinsic tyrosine fluorescence shows a sigmoidal transition, indicating that L is most likely a thermodynamic state separated from U with a distinct free energy barrier. Hence, the U ↔ L transition was modeled as a two-state transition.

It must, however, be noted that a sigmoidal burst phase transition does not always imply a cooperative two-state transition.[30,78,84,85] In fact, the dependence of the amplitude for the early intermediate L using ANS fluorescence suggests that the U ↔ L transition may be a noncooperative transition (Figure 4D, inset). Moreover, in an earlier study of the refolding of the PI3K SH3 domain in the absence of any stabilizing cosolute, the sub-millisecond formation of the structure-less globule U_C was shown, using multisite FRET measurements, to be a gradual process, similar to a coil to globule transition.[41] In this respect, the sub-millisecond folding reaction of the PI3K SH3 domain therefore appears to be similar to that of barstar,[30,85,86] for which the utilization of multiple structural probes had suggested that the sub-millisecond formation of a structure-less globule (analogous to U_C) as well as of a very early folding intermediate (analogous to L) occurred as barrier-less ($<3k_BT$) transitions. Under strongly stabilizing conditions, the sub-millisecond folding transition of barstar becomes more sigmoidal, but the transition clearly remains noncooperative because the sigmoidal transitions measured by different probes are noncoincident.[50] It remains to be seen if the sigmoidal transition observed for the PI3K SH3 domain represents a gradual or all-or-none transition under all folding conditions or whether stabilization of the folding conditions results in a tuning of the free energy landscape from one with many small distributed barriers to one with a single dominant barrier. This is an important question to address in future studies, and while it is difficult to distinguish experimentally an all-or-none folding transition from a continuous one,[87,88] a growing body of evidence suggests that for several proteins from single-molecule FRET studies[38,89,90] the transition of the unfolded state to a collapsed form is gradual in nature.

Refolding Leads Initially to the Formation of a Non-specific U_C and a Specific L. The millisecond refolding mechanism of the PI3K SH3 domain in the absence of a cosolute has been delineated.[41] The ensemble of non-specific compact intermediates (U_C) reported in that study showed weak ANS binding, a non-specific contraction of three intramolecular distances at low denaturant concentrations and appeared to be devoid of significant secondary structure. In this study, it is shown that L is a distinct state that is populated within milliseconds of the initiation of the refolding reaction in the presence of 0.5 M Na_2SO_4.

Both U_C in the absence and L in the presence of 0.5 M Na_2SO_4 exhibit properties of a molten globule in that they bind to ANS. ANS is a dye that has both polarity and hydrophobicity. The presence of both polar and apolar groups in the molecule helps it bind to partially structured forms populated in the kinetic pathways of proteins.[21,66,67,91,92] In investigating the refolding of the PI3K SH3 domain, the larger increase in ANS fluorescence due to binding to L in the presence of 0.5 M Na_2SO_4 relative to that reported previously for U_C[41] suggests an increase in the specific sites available for the ANS binding in the presence of 0.5 M Na_2SO_4. The enhanced binding of ANS is probably due to the greater structural content of L. For example, ANS has been shown to have a significantly higher affinity for the β-structural conformation of a polypeptide chain relative to the α-helical structure.[91] A value of 0.5 for α_L, the relative position of L on the reaction coordinate (Table 1), suggests that L is 50% as compact as N. Moreover, FRET studies indicate specific contraction of two intramolecular distances in the L ensemble (data not shown). These observations suggest that the addition of salt preferentially stabilizes a structured component of the initially collapsed ensemble in the refolding of the PI3K SH3 domain. Such specific components of the collapsed ensemble have been reported in the folding of other proteins too.[44,86,93]

It appears that L and U_C are part of the same collapsed ensemble, where L is a structured intermediate and U_C is unstructured. With the addition of Na_2SO_4, conditions become favorable for stabilizing the structured component, L, sufficiently for it to be detectable by the probes used in this study (Figure 6). In the case of barstar, it was shown that different salts[42] as well as osmolytes[50] differentially stabilize different components of the collapsed ensemble that forms initially during folding. At present, it is not known whether U_C and L in the case of the PI3K SH3 domain are separated by a

dx.doi.org/10.1021/bi300223b | Biochemistry 2012, 51, 4723−4734

free energy barrier. Sub-millisecond folding experiments, now in progress, will address this important issue.

An unusual result of the four-state analysis is that the value of m^S_{LU} [−1.55 kcal mol^{-1} M^{-1} (Table 1)] is substantially larger than that of m^S_{ML} [−0.7 kcal mol^{-1} M^{-1} (Table 1)], indicating that more surface area is buried during the early folding step (U to L) than during the rate-limiting step (L to M). This result is somewhat surprising, but it should be noted that the m^S values listed in Table 1 are robust because they have been determined from the dependence on GdnHCl concentration of the amplitude of the sub-millisecond folding reaction and of the amplitude of the sub-millisecond unfolding reaction (eqs 1, 8, and 9). It is possible that the large m^S_{LU} value for the U to L transition is a reflection of this transition being noncooperative in nature, perhaps even gradual (see above).

Unfolding Mechanism in the Presence of 0.5 M Na_2SO_4. Detailed studies of the unfolding mechanism of the PI3K SH3 domain using optical probes and HX-MS in urea and GdnHCl have indicated the presence of partially unfolded forms on two parallel pathways.[20,57] At high concentrations of GdnHCl, the formation of an unfolding intermediate, I_U, that has U-like intrinsic tyrosine fluorescence properties was reported using optical probes to monitor unfolding in the absence of any added salt.[57] In our study, an unfolding intermediate M was detected only at high GdnHCl concentrations in the presence of 0.5 M Na_2SO_4 by the use of the same optical probes. It is therefore highly likely that M and I_U are the same intermediates, and that the unfolding pathway is not altered by the addition of 0.5 M Na_2SO_4, at high GdnHCl concentrations.

It is possible that the transition from N to M may not be barrier-limited, as has been assumed in Scheme 1, but that it is, instead, a barrier-less transition. The observation that the content of secondary structure of the protein changes upon addition of Na_2SO_4 suggests that the structure of the native state of the protein is malleable, and the sub-millisecond transition from N to M may reflect an adjustment of the native state to a change from native to unfolding conditions. It is possible that N undergoes a gradual, diffusive conversion to M over many small distributed free energy barriers as has been theoretically reported for the swelling of molten globule states.[94] A gradual structural change during unfolding can be detected using high-resolution techniques in equilibrium unfolding experiments,[39,43,95−98] as well as in kinetic unfolding studies.[19]

Nature of the Rate-Limiting Transition State (TS2) for Folding. Figure 6 shows the free energy profiles for the four-state folding of the PI3K SH3 domain in the presence and absence of 0.5 M Na_2SO_4 in 0 and 5 M GdnHCl constructed from the values listed in Table 1. The reaction coordinate is α, which can be considered as a measure for the extent of folding in L and M compared to that in N.[57] L is populated before the rate-limiting step, and it is 50% as compact as N. On the other hand, M is populated only after the rate-limiting step for the folding reaction and hence can be detected only in unfolding experiments. From the fits to the quantitative four-state model, it is seen that M is ∼70% folded in the presence of 0.5 M Na_2SO_4.

The ANS binding amplitude of L is greater than the ANS binding amplitude observed for M. As already mentioned, M is not populated to a significant extent during folding, and similarly L during unfolding, yet it seems that as the folding proceeds from L to N via M, the hydrophobic patches that are exposed in L may begin to consolidate into the hydrophobic core in M, resulting in a lower ANS binding capacity. As M proceeds to N, the hydrophobic core is formed completely and the ANS is released from the protein. Thus, from the values of α for L and M and the ANS binding experiments, it seems that TS2 is considerably compact and is partially hydrated.

Can L or M Be Off-Pathway Intermediates? Kinetic analyses cannot usually determine whether an initial intermediate formed rapidly in pre-equilibrium with U or N is on-pathway or off-pathway.[99] Indeed, this has been a problem in the interpretation of kinetic studies of the folding of several proteins.[21,47,64,65,100] In this study, the possibility of L being a dead-end intermediate as depicted in Scheme 2 cannot be

Scheme 2

$$L \rightleftharpoons U \rightleftharpoons M \rightleftharpoons N$$

completely ruled out, because the fit of the data to Scheme 2 (fit not shown) is as good as that to Scheme 1. No roll-down is observed in the folding arm of the chevron, as might be expected for Scheme 2 when the unfolding of L to U becomes rate-limiting in the formation of N at low denaturant concentrations where L accumulates.[49,101] On the other hand, the observation that both L and N are stabilized by the addition of Na_2SO_4 is consistent with L being a productive on-pathway intermediate possessing native-like structure. Moreover, the observation that the rate of folding to N increases with an increase in Na_2SO_4 concentration is consistent with the rate-limiting TS occurring after a native-like L on the direct folding pathway, because it too would then be stabilized upon addition of Na_2SO_4.

Because the transition from N to M can also be approximated as a pre-equilibrium in the kinetic analysis, on the basis of the observation that M is rapidly formed from N and that further unfolding of M is slow, the possibility of M being off-pathway to N according to Scheme 3 cannot similarly

Scheme 3

$$U \rightleftharpoons L \rightleftharpoons N \rightleftharpoons M$$

be ruled out. In fact, the data in Figure 5 also fit well to Scheme 3 (not shown), but the observation that the initial pre-equilibrium established between N and M at the start of unfolding is not perturbed by the presence of 0.5 M Na_2SO_4 (Figure 4C)[57] indicates that M becomes stabilized to the same extent as N does, by the addition of Na_2SO_4. Hence, M must possess much of the structure present in N, as expected for an on-pathway intermediate, and not for an off-pathway intermediate. M is also seen in equilibrium unfolding studies in the absence of Na_2SO_4, and an m value analysis had indicated that M is on the direct unfolding pathway.[57]

Properties of the M Ensemble. The observation that M becomes stabilized to the same extent as N upon addition of 0.5 M Na_2SO_4 (Table 1 and Figure 6) suggests that the Hofmeister effect plays a dominant role in the salt-induced stabilization of M, too, as it does for N (see above). In fact, a slight increase in the value of α_M, from 0.6 in the absence of salt[57] to 0.7 in the presence of 0.5 M Na_2SO_4 (Table 1), is observed, indicating a greater burial of solvent accessible surface area in the presence of the salt.

dx.doi.org/10.1021/bi300223b | Biochemistry 2012, 51, 4723−4734

It appears that the fluorescence properties of M change upon going from refolding to unfolding conditions. Under strongly unfolding conditions, M possesses tyrosine fluorescence properties identical to those of the U state (see Figure 4C), but if this were the case even under refolding conditions, it would imply that during folding the intrinsic tyrosine fluorescence of U first decreases in L and then increases in M and finally decreases again in N. It is important to note here that M is populated only after the rate-limiting step of folding, and it therefore cannot be detected under refolding conditions. Hence, it cannot be established whether the fluorescence properties of M are actually different under refolding conditions or whether the fluorescence decreases monotonously during refolding only because M is so scarcely populated.

If the fluorescence properties of the M ensemble do change with a change in folding versus unfolding conditions, it could be because M contains subpopulations of different conformations in equilibrium with each other, and a different subpopulation is stabilized under different conditions. Moreover, if there are several subpopulations, there may be independent unfolding pathways operating under different folding conditions.[24] In fact, native state HX studies of the unfolding of the SH3 domain of PI3K showed that the unfolding in the absence of GdnHCl and at low concentrations of GdnHCl is initiated via the formation of another intermediate, I_N,[20] which has N-like protection of amide hydrogens and N-like fluorescence and hence is undetected in optical studies.[57] It may be possible that under refolding conditions, a subpopulation of M that resembles I_N in its structural properties is populated but is undetected with the set of probes used in this study. Such structural heterogeneity has been elucidated in the unfolding of the late folding intermediate, I_L, of barstar using multisite TR-FRET.[18]

In the future, it will be interesting to investigate the structural properties of L and M using a high-resolution, site-specific probe such as multisite FRET to gather useful information about the structural heterogeneity inherent to folding intermediates populated both before and after the rate-limiting step. Moreover, sub-millisecond studies will also shed light on the nature of transitions that lead to the formation of such structurally distinct states. Such experiments are currently ongoing in our laboratory.

AUTHOR INFORMATION

Corresponding Author

*E-mail: jayant@ncbs.res.in. Phone: 91-80-23666150. Fax: 91-80-23636662.

Funding

This work was funded by the Tata Institute of Fundamental Research and by the Department of Science and Technology, Government of India. J.B.U. is a recipient of the J. C. Bose National Fellowship from the Government of India.

Notes

The authors declare no competing financial interest.

ACKNOWLEDGMENTS

We thank all the members of our laboratory for discussions.

ABBREVIATIONS

ANS, 1-anilinonaphthalene-8-sulfonate; CD, circular dichroism; FRET, fluorescence resonance energy transfer; PI3K SH3, SH3 domain of PI3 kinase.

REFERENCES

(1) Jackson, S. E. (1998) How do small single-domain proteins fold? *Folding Des. 3*, R81−R91.

(2) Plaxco, K. W., Simons, K. T., and Baker, D. (1998) Contact order, transition state placement and the refolding rates of single domain proteins. *J. Mol. Biol. 277*, 985−994.

(3) Miller, E. J., Fischer, K. F., and Marqusee, S. (2002) Experimental evaluation of topological parameters determining protein-folding rates. *Proc. Natl. Acad. Sci. U.S.A. 99*, 10359−10363.

(4) Gromiha, M. M. (2005) A statistical model for predicting protein folding rates from amino acid sequence with structural class information. *J. Chem. Inf. Model. 45*, 494−501.

(5) Li, M. S., Klimov, D. K., and Thirumalai, D. (2004) Finite size effects on thermal denaturation of globular proteins. *Phys. Rev. Lett. 93*, 268107.

(6) Naganathan, A. N., and Munoz, V. (2005) Scaling of folding times with protein size. *J. Am. Chem. Soc. 127*, 480−481.

(7) Dinner, A. R., and Karplus, M. (2001) The roles of stability and contact order in determining protein folding rates. *Nat. Struct. Biol. 8*, 21−22.

(8) Fersht, A. R. (1995) Characterizing transition states in protein folding: An essential step in the puzzle. *Curr. Opin. Struct. Biol. 5*, 79−84.

(9) Zarrine-Afsar, A., Dahesh, S., and Davidson, A. R. (2012) A residue in helical conformation in the native state adopts a β-strand conformation in the folding transition state despite its high and canonical ϕ-value. *Proteins 80*, 1343−1349.

(10) Li, L., Mirny, L. A., and Shakhnovich, E. I. (2000) Kinetics, thermodynamics and evolution of non-native interactions in a protein folding nucleus. *Nat. Struct. Biol. 7*, 336−342.

(11) Klimov, D. K., and Thirumalai, D. (2002) Stiffness of the distal loop restricts the structural heterogeneity of the transition state ensemble in SH3 domains. *J. Mol. Biol. 317*, 721−737.

(12) Paci, E., Lindorff-Larsen, K., Dobson, C. M., Karplus, M., and Vendruscolo, M. (2005) Transition state contact orders correlate with protein folding rates. *J. Mol. Biol. 352*, 495−500.

(13) Go, N. (1983) Theoretical studies of protein folding. *Annu. Rev. Biophys. Bioeng. 12*, 183−210.

(14) Onuchic, J. N., Luthey-Schulten, Z., and Wolynes, P. G. (1997) Theory of protein folding: The energy landscape perspective. *Annu. Rev. Phys. Chem. 48*, 545−600.

(15) Bryngelson, J. D., Onuchic, J. N., Socci, N. D., and Wolynes, P. G. (1995) Funnels, pathways, and the energy landscape of protein folding: A synthesis. *Proteins 21*, 167−195.

(16) Lakshmikanth, G. S., Sridevi, K., Krishnamoorthy, G., and Udgaonkar, J. B. (2001) Structure is lost incrementally during the unfolding of barstar. *Nat. Struct. Biol. 8*, 799−804.

(17) Mello, C. C., and Barrick, D. (2004) An experimentally determined protein folding energy landscape. *Proc. Natl. Acad. Sci. U.S.A. 101*, 14102−14107.

(18) Sridevi, K., Lakshmikanth, G. S., Krishnamoorthy, G., and Udgaonkar, J. B. (2004) Increasing stability reduces conformational heterogeneity in a protein folding intermediate ensemble. *J. Mol. Biol. 337*, 699−711.

(19) Jha, S. K., Dhar, D., Krishnamoorthy, G., and Udgaonkar, J. B. (2009) Continuous dissolution of structure during the unfolding of a small protein. *Proc. Natl. Acad. Sci. U.S.A. 106*, 11113−11118.

(20) Wani, A. H., and Udgaonkar, J. B. (2009) Native state dynamics drive the unfolding of the SH3 domain of PI3 kinase at high denaturant concentration. *Proc. Natl. Acad. Sci. U.S.A. 106*, 20711−20716.

(21) Shastry, M. C., and Udgaonkar, J. B. (1995) The folding mechanism of barstar: Evidence for multiple pathways and multiple intermediates. *J. Mol. Biol. 247*, 1013−1027.

(22) Bhuyan, A. K., and Udgaonkar, J. B. (1999) Observation of multistate kinetics during the slow folding and unfolding of barstar. *Biochemistry 38*, 9158−9168.

(23) Patra, A. K., and Udgaonkar, J. B. (2007) Characterization of the folding and unfolding reactions of single-chain monellin: Evidence for

multiple intermediates and competing pathways. *Biochemistry 46*, 11727−11743.
(24) Udgaonkar, J. B. (2008) Multiple routes and structural heterogeneity in protein folding. *Annu. Rev. Biophys. 37*, 489−510.
(25) Jha, S. K., Dasgupta, A., Malhotra, P., and Udgaonkar, J. B. (2011) Identification of multiple folding pathways of monellin using pulsed thiol labeling and mass spectrometry. *Biochemistry 50*, 3062−3074.
(26) Garcia-Mira, M. M., Sadqi, M., Fischer, N., Sanchez-Ruiz, J. M., and Munoz, V. (2002) Experimental identification of downhill protein folding. *Science 298*, 2191−2195.
(27) Gruebele, M. (2005) Downhill protein folding: Evolution meets physics. *C. R. Biol. 328*, 701−712.
(28) Munoz, V. (2007) Conformational dynamics and ensembles in protein folding. *Annu. Rev. Biophys. Biomol. Struct. 36*, 395−412.
(29) Eaton, W. A. (1999) Searching for "downhill scenarios" in protein folding. *Proc. Natl. Acad. Sci. U.S.A. 96*, 5897−5899.
(30) Sinha, K. K., and Udgaonkar, J. B. (2008) Barrierless evolution of structure during the submillisecond refolding reaction of a small protein. *Proc. Natl. Acad. Sci. U.S.A. 105*, 7998−8003.
(31) Munoz, V. (2002) Thermodynamics and kinetics of downhill protein folding investigated with a simple statistical mechanical model. *Int. J. Quantum Chem. 90*, 1522−1528.
(32) Lei, H., Wu, C., Liu, H., and Duan, Y. (2007) Folding free-energy landscape of villin headpiece subdomain from molecular dynamics simulations. *Proc. Natl. Acad. Sci. U.S.A. 104*, 4925−4930.
(33) Piana, S., Sarkar, K., Lindorff-Larsen, K., Guo, M., Gruebele, M., and Shaw, D. E. (2010) Computational design and experimental testing of the fastest-folding β-sheet protein. *J. Mol. Biol. 405*, 43−48.
(34) Shaw, D. E., Maragakis, P., Lindorff-Larsen, K., Piana, S., Dror, R. O., Eastwood, M. P., Bank, J. A., Jumper, J. M., Salmon, J. K., Shan, Y., and Wriggers, W. (2010) Atomic-level characterization of the structural dynamics of proteins. *Science 330*, 341−346.
(35) Lindorff-Larsen, K., Piana, S., Dror, R. O., and Shaw, D. E. (2011) How fast-folding proteins fold. *Science 334*, 517−520.
(36) Noe, F., Schutte, C., Vanden-Eijnden, E., Reich, L., and Weikl, T. R. (2009) Constructing the equilibrium ensemble of folding pathways from short off-equilibrium simulations. *Proc. Natl. Acad. Sci. U.S.A. 106*, 19011−19016.
(37) Bowman, G. R., and Pande, V. S. (2010) Protein folded states are kinetic hubs. *Proc. Natl. Acad. Sci. U.S.A. 107*, 10890−10895.
(38) Schuler, B., Lipman, E. A., and Eaton, W. A. (2002) Probing the free-energy surface for protein folding with single-molecule fluorescence spectroscopy. *Nature 419*, 743−747.
(39) Sadqi, M., Fushman, D., and Munoz, V. (2006) Atom-by-atom analysis of global downhill protein folding. *Nature 442*, 317−321.
(40) Jha, S. K., and Udgaonkar, J. B. (2007) Exploring the cooperativity of the fast folding reaction of a small protein using pulsed thiol labeling and mass spectrometry. *J. Biol. Chem. 282*, 37479−37491.
(41) Dasgupta, A., and Udgaonkar, J. B. (2010) Evidence for initial non-specific polypeptide chain collapse during the refolding of the SH3 domain of PI3 kinase. *J. Mol. Biol. 403*, 430−445.
(42) Pradeep, L., and Udgaonkar, J. B. (2002) Differential salt-induced stabilization of structure in the initial folding intermediate ensemble of barstar. *J. Mol. Biol. 324*, 331−347.
(43) Rami, B. R., and Udgaonkar, J. B. (2002) Mechanism of formation of a productive molten globule form of barstar. *Biochemistry 41*, 1710−1716.
(44) Magg, C., Kubelka, J., Holtermann, G., Haas, E., and Schmid, F. X. (2006) Specificity of the initial collapse in the folding of the cold shock protein. *J. Mol. Biol. 360*, 1067−1080.
(45) Nath, U., and Udgaonkar, J. B. (1995) Perturbation of a tertiary hydrogen bond in barstar by mutagenesis of the sole His residue to Gln leads to accumulation of at least one equilibrium folding intermediate. *Biochemistry 34*, 1702−1713.
(46) Connell, K. B., Horner, G. A., and Marqusee, S. (2009) A single mutation at residue 25 populates the folding intermediate of *E. coli* RNase H and reveals a highly dynamic partially folded ensemble. *J. Mol. Biol. 391*, 461−470.
(47) Khorasanizadeh, S., Peters, I. D., and Roder, H. (1996) Evidence for a three-state model of protein folding from kinetic analysis of ubiquitin variants with altered core residues. *Nat. Struct. Biol. 3*, 193−205.
(48) Bieri, O., Wildegger, G., Bachmann, A., Wagner, C., and Kiefhaber, T. (1999) A salt-induced kinetic intermediate is on a new parallel pathway of lysozyme folding. *Biochemistry 38*, 12460−12470.
(49) Otzen, D. E., and Oliveberg, M. (1999) Salt-induced detour through compact regions of the protein folding landscape. *Proc. Natl. Acad. Sci. U.S.A. 96*, 11746−11751.
(50) Pradeep, L., and Udgaonkar, J. B. (2004) Osmolytes induce structure in an early intermediate on the folding pathway of barstar. *J. Biol. Chem. 279*, 40303−40313.
(51) Jahn, T. R., Parker, M. J., Homans, S. W., and Radford, S. E. (2006) Amyloid formation under physiological conditions proceeds via a native-like folding intermediate. *Nat. Struct. Mol. Biol. 13*, 195−201.
(52) Neudecker, P., Robustelli, P., Cavalli, A., Walsh, P., Lundstrom, P., Zarrine-Afsar, A., Sharpe, S., Vendruscolo, M., and Kay, L. E. (2012) Structure of an intermediate state in protein folding and aggregation. *Science 336*, 362−366.
(53) Roder, H., and Colon, W. (1997) Kinetic role of early intermediates in protein folding. *Curr. Opin. Struct. Biol. 7*, 15−28.
(54) Jha, S. K., and Udgaonkar, J. B. (2009) Direct evidence for a dry molten globule intermediate during the unfolding of a small protein. *Proc. Natl. Acad. Sci. U.S.A. 106*, 12289−12294.
(55) Goldenberg, D. P., and Creighton, T. E. (1985) Energetics of protein structure and folding. *Biopolymers 24*, 167−182.
(56) Agashe, V. R., Schmid, F. X., and Udgaonkar, J. B. (1997) Thermodynamics of the complex protein unfolding reaction of barstar. *Biochemistry 36*, 12288−12295.
(57) Wani, A. H., and Udgaonkar, J. B. (2009) Revealing a concealed intermediate that forms after the rate-limiting step of refolding of the SH3 domain of PI3 kinase. *J. Mol. Biol. 387*, 348−362.
(58) Wani, A. H., and Udgaonkar, J. B. (2006) HX-ESI-MS and optical studies of the unfolding of thioredoxin indicate stabilization of a partially unfolded, aggregation-competent intermediate at low pH. *Biochemistry 45*, 11226−11238.
(59) Baldwin, R. L., Frieden, C., and Rose, G. D. (2010) Dry molten globule intermediates and the mechanism of protein unfolding. *Proteins 78*, 2725−2737.
(60) Bai, Y., Sosnick, T. R., Mayne, L., and Englander, S. W. (1995) Protein folding intermediates: Native-state hydrogen exchange. *Science 269*, 192−197.
(61) Juneja, J., and Udgaonkar, J. B. (2002) Characterization of the unfolding of ribonuclease A by a pulsed hydrogen exchange study: Evidence for competing pathways for unfolding. *Biochemistry 41*, 2641−2654.
(62) Guijarro, J. I., Morton, C. J., Plaxco, K. W., Campbell, I. D., and Dobson, C. M. (1998) Folding kinetics of the SH3 domain of PI3 kinase by real-time NMR combined with optical spectroscopy. *J. Mol. Biol. 276*, 657−667.
(63) Bader, R., Bamford, R., Zurdo, J., Luisi, B. F., and Dobson, C. M. (2006) Probing the mechanism of amyloidogenesis through a tandem repeat of the PI3-SH3 domain suggests a generic model for protein aggregation and fibril formation. *J. Mol. Biol. 356*, 189−208.
(64) Sauder, J. M., MacKenzie, N. E., and Roder, H. (1996) Kinetic mechanism of folding and unfolding of *Rhodobacter capsulatus* cytochrome c2. *Biochemistry 35*, 16852−16862.
(65) Fersht, A. R. (2000) A kinetically significant intermediate in the folding of barnase. *Proc. Natl. Acad. Sci. U.S.A. 97*, 14121−14126.
(66) Stryer, L. (1965) The interaction of a naphthalene dye with apomyoglobin and apohemoglobin. A fluorescent probe of non-polar binding sites. *J. Mol. Biol. 13*, 482−495.
(67) Agashe, V. R., Shastry, M. C., and Udgaonkar, J. B. (1995) Initial hydrophobic collapse in the folding of barstar. *Nature 377*, 754−757.

(68) Sridevi, K., Juneja, J., Bhuyan, A. K., Krishnamoorthy, G., and Udgaonkar, J. B. (2000) The slow folding reaction of barstar: The core tryptophan region attains tight packing before substantial secondary and tertiary structure formation and final compaction of the polypeptide chain. *J. Mol. Biol. 302*, 479−495.
(69) Von Hippel, P. H., and Wong, K. Y. (1965) On the conformational stability of globular proteins. The effects of various electrolytes and nonelectrolytes on the thermal ribonuclease transition. *J. Biol. Chem. 240*, 3909−3923.
(70) Arakawa, T., and Timasheff, S. N. (1982) Preferential interactions of proteins with salts in concentrated solutions. *Biochemistry 21*, 6545−6552.
(71) Lindman, S., Xue, W. F., Szczepankiewicz, O., Bauer, M. C., Nilsson, H., and Linse, S. (2006) Salting the charged surface: pH and salt dependence of protein G B1 stability. *Biophys. J. 90*, 2911−2921.
(72) Baldwin, R. L. (1996) How Hofmeister ion interactions affect protein stability. *Biophys. J. 71*, 2056−2063.
(73) Ramos, C. H., and Baldwin, R. L. (2002) Sulfate anion stabilization of native ribonuclease A both by anion binding and by the Hofmeister effect. *Protein Sci. 11*, 1771−1778.
(74) Collins, K. D., and Washabaugh, M. W. (1985) The Hofmeister effect and the behaviour of water at interfaces. *Q. Rev. Biophys. 18*, 323−422.
(75) Schellman, J. A. (1990) A simple model for solvation in mixed solvents. Applications to the stabilization and destabilization of macromolecular structures. *Biophys. Chem. 37*, 121−140.
(76) Record, M. T., Jr., Zhang, W., and Anderson, C. F. (1998) Analysis of effects of salts and uncharged solutes on protein and nucleic acid equilibria and processes: A practical guide to recognizing and interpreting polyelectrolyte effects, Hofmeister effects, and osmotic effects of salts. *Adv. Protein Chem. 51*, 281−353.
(77) de Los Rios, M. A., and Plaxco, K. W. (2005) Apparent Debye-Huckel electrostatic effects in the folding of a simple, single domain protein. *Biochemistry 44*, 1243−1250.
(78) Chan, H. S., Bromberg, S., and Dill, K. A. (1995) Models of cooperativity in protein folding. *Philos. Trans. R. Soc. London, Ser. B 348*, 61−70.
(79) Klimov, D. K., and Thirumalai, D. (2002) Is there a unique melting temperature for two-state proteins? *J. Comput. Chem. 23*, 161−165.
(80) Abkevich, V. I., Gutin, A. M., and Shakhnovich, E. I. (1995) Impact of local and non-local interactions on thermodynamics and kinetics of protein folding. *J. Mol. Biol. 252*, 460−471.
(81) Poland, D. C., and Scheraga, H. A. (1965) Statistical Mechanics of Noncovalent Bonds in Polyamino Acids. IX. 2-State Theory of Protein Denaturation. *Biopolymers 3*, 401−419.
(82) Desai, T. M., Cerminara, M., Sadqi, M., and Munoz, V. (2010) The effect of electrostatics on the marginal cooperativity of an ultrafast folding protein. *J. Biol. Chem. 285*, 34549−34556.
(83) Luo, Y., Kay, M. S., and Baldwin, R. L. (1997) Cooperativity of folding of the apomyoglobin pH 4 intermediate studied by glycine and proline mutations. *Nat. Struct. Biol. 4*, 925−930.
(84) Parker, M. J., and Marqusee, S. (1999) The cooperativity of burst phase reactions explored. *J. Mol. Biol. 293*, 1195−1210.
(85) Sinha, K. K., and Udgaonkar, J. B. (2005) Dependence of the size of the initially collapsed form during the refolding of barstar on denaturant concentration: Evidence for a continuous transition. *J. Mol. Biol. 353*, 704−718.
(86) Sinha, K. K., and Udgaonkar, J. B. (2007) Dissecting the non-specific and specific components of the initial folding reaction of barstar by multi-site FRET measurements. *J. Mol. Biol. 370*, 385−405.
(87) Huang, F., Sato, S., Sharpe, T. D., Ying, L., and Fersht, A. R. (2007) Distinguishing between cooperative and unimodal downhill protein folding. *Proc. Natl. Acad. Sci. U.S.A. 104*, 123−127.
(88) Naganathan, A. N., Doshi, U., and Munoz, V. (2007) Protein folding kinetics: Barrier effects in chemical and thermal denaturation experiments. *J. Am. Chem. Soc. 129*, 5673−5682.
(89) Sherman, E., and Haran, G. (2006) Coil-globule transition in the denatured state of a small protein. *Proc. Natl. Acad. Sci. U.S.A. 103*, 11539−11543.
(90) Merchant, K. A., Best, R. B., Louis, J. M., Gopich, I. V., and Eaton, W. A. (2007) Characterizing the unfolded states of proteins using single-molecule FRET spectroscopy and molecular simulations. *Proc. Natl. Acad. Sci. U.S.A. 104*, 1528−1533.
(91) Semisotnov, G. V., Rodionova, N. A., Razgulyaev, O. I., Uversky, V. N., Gripas, A. F., and Gilmanshin, R. I. (1991) Study of the "molten globule" intermediate state in protein folding by a hydrophobic fluorescent probe. *Biopolymers 31*, 119−128.
(92) Engelhard, M., and Evans, P. A. (1995) Kinetics of interaction of partially folded proteins with a hydrophobic dye: Evidence that molten globule character is maximal in early folding intermediates. *Protein Sci. 4*, 1553−1562.
(93) Kimura, T., Uzawa, T., Ishimori, K., Morishima, I., Takahashi, S., Konno, T., Akiyama, S., and Fujisawa, T. (2005) Specific collapse followed by slow hydrogen-bond formation of β-sheet in the folding of single-chain monellin. *Proc. Natl. Acad. Sci. U.S.A. 102*, 2748−2753.
(94) Finkelstein, A. V., and Shakhnovich, E. I. (1989) Theory of cooperative transitions in protein molecules. II. Phase diagram for a protein molecule in solution. *Biopolymers 28*, 1681−1694.
(95) O'Brien, R., Sturtevant, J. M., Wrabl, J., Holtzer, M. E., and Holtzer, A. (1996) A scanning calorimetric study of unfolding equilibria in homodimeric chicken gizzard tropomyosins. *Biophys. J. 70*, 2403−2407.
(96) Swaminathan, R., Nath, U., Udgaonkar, J. B., Periasamy, N., and Krishnamoorthy, G. (1996) Motional dynamics of a buried tryptophan reveals the presence of partially structured forms during denaturation of barstar. *Biochemistry 35*, 9150−9157.
(97) Rami, B. R., Krishnamoorthy, G., and Udgaonkar, J. B. (2003) Dynamics of the core tryptophan during the formation of a productive molten globule intermediate of barstar. *Biochemistry 42*, 7986−8000.
(98) Ahmed, Z., Beta, I. A., Mikhonin, A. V., and Asher, S. A. (2005) UV-resonance Raman thermal unfolding study of Trp-cage shows that it is not a simple two-state miniprotein. *J. Am. Chem. Soc. 127*, 10943−10950.
(99) Baldwin, R. L. (1996) On-pathway versus off-pathway folding intermediates. *Folding Des. 1*, R1−R8.
(100) Wildegger, G., and Kiefhaber, T. (1997) Three-state model for lysozyme folding: Triangular folding mechanism with an energetically trapped intermediate. *J. Mol. Biol. 270*, 294−304.
(101) Bhuyan, A. K., and Udgaonkar, J. B. (2001) Folding of horse cytochrome c in the reduced state. *J. Mol. Biol. 312*, 1135−1160.
(102) Pettersen, E. F., Goddard, T. D., Huang, C. C., Couch, G. S., Greenblatt, D. M., Meng, E. C., and Ferrin, T. E. (2004) UCSF Chimera: A visualization system for exploratory research and analysis. *J. Comput. Chem. 25*, 1605−1612.